EASR

Engineering and Applied Science Research

https://www.tci-thaijo.org/index.php/easr/index

Published by the Faculty of Engineering, Khon Kaen University, Thailand

Preparation and mechanism analysis of morphology-controlled cellulose nanocrystals by H_2SO_4 hydrolysis of *Eucalyptus* pulp

Pasakorn Jutakridsada[1)], Somnuk Theerakulpisut[2)], Varsha Srivastava[3)], Mika Sillanpää[4)] and Khanita Kamwilaisak*[1)]

[1)]Department of Chemical Engineering, Faculty of Engineering, Khon Kaen University, Khon Kaen 40002, Thailand
[2)]Energy Management and Conservation Office, Khon Kaen University, Khon Kaen 40002, Thailand
[3)]Department of Separation Science, School of Engineering Science, Lappeenranta-Lahti University of Technology LUT, Sammonkatu 12, 50130 Mikkeli, Finland
[4)]Department Chemistry, College of Science, King Saud University, Riyadh 11451, Saudi Arabia

Received 21 August 2022
Revised 19 November 2022
Accepted 25 November 2022

Abstract

Cellulose from *Eucalyptus* pulp has been used as raw material for producing cellulose nanocrystals (CNCs). In this research work, H_2SO_4 hydrolysis was utilized in the production of CNCs. The effects of hydrolysis parameters, namely, H_2SO_4 concentration (30, 40, and 50 wt%), hydrolysis time (30, 60, and 90 min), and hydrolysis temperature (60, 70, and 80 °C), on the CNC structure were examined. The physical and chemical properties of *Eucalyptus* pulp and CNCs were characterized using different techniques such as X-ray diffraction (XRD), Fourier-transform infrared spectroscopy (FT-IR), scanning electron microscopy (SEM), transmittance electron microscopy (TEM), and thermal gravimetric analysis (TGA). The results showed the optimal condition was at 50 wt% of H_2SO_4 concentration, 60 min hydrolysis time, and 60 °C hydrolysis temperature, which yielded 75.51% ± 1.51 % of crystallinity and 4.03 ± 0.10 nm of crystal size. Furthermore, it was also determined that an increase in H_2SO_4 concentration, time, or temperature led to a lower percentage of crystallinity and reduction in crystal size. CNCs were noted to be more thermally stable than the *Eucalyptus* pulp. Thus, this method could be an alternative way to create a new product in the paper industry.

Keywords: Cellulose nanocrystals, *Eucalyptus* pulp, H_2SO_4 hydrolysis

1. Introduction

Eucalyptus pulp is a known product from a pulping process of *Eucalyptus* wood. It is a major feedstock for paper industry in Thailand and across the world; this is because *Eucalyptus* is a rapid growing softwood species with high fiber qualities and of low market price due to decreasing demand for paper. Thus, to seek out and add value to the *Eucalyptus* pulp by making alternative uses of it would be an interesting topic [1, 2]. Preparation of cellulose nanocrystals (CNCs) from *Eucalyptus* pulp is an interesting choice due to CNCs having several attractive properties such as their high specific strength, high surface area, hydrophilicity, and biocompatibility [3, 4]. Therefore, CNCs have attracted attention for its application in various fields such as food, paper, and medicine [1, 5]. In addition, CNCs were also widely incorporated into a polymer matrix to reinforce the mechanical strength of polymer-based nanocomposites [6, 7]. To obtain CNCs, mechanical (refining, sonication, stone grinder, and high-pressure homogenizer) and chemical (acid hydrolysis and TEMPO) methods are commonly used to produce CNCs from *Eucalyptus* pulp. For example, Zhao et al. [8] prepared cellulose nanofibrils (CNFs) with diameters in the range of 15-40 nm by combining physical methods of ultrasonic treatment and high shear homogenization and then produced nanocomposite films with varying the CNFs. The nanocomposite film showed good optical transparency, thermal stability, and remarkably enhanced mechanical properties compared to the regenerated cellulose matrix. Besbes et al. [9] reported the preparation of CNCs by using an oxidation pretreatment method. 2, 2, 6, 6,-Tetramethylpiperidine-1-oxyl radical (TEMPO) was used as a mediator at 60 °C for 2 to 72 h; then, defibrillation process was applied under pressure of 600 bar. This method yielded the nanofibrillated celluloses over 90% with 18-19 µm in diameter and 625-645 µm in length. The obtained CNCs had rod-like particles with approximately 250 nm in length and 20 nm in diameter and single nanocrystal with a diameter of 3-5 nm.

An acid hydrolysis has been identified as an alternative method to produce the CNCs, and three mineral acids, namely, hydrochloric acid, phosphoric acid, and sulfuric acid, are commonly used [10]. However, hydrolysis using sulfuric acid is an interesting choice due to the obtained CNCs having an anionic sulfate half esters ($-OSO^-_3$) on the surface resulting in high negative zeta potential and colloidal stability in aqueous solution [1, 7, 11].

Several studies have reported the use of sulfuric acid hydrolysis to produce CNCs from *Eucalyptus* pulp. For example, Carvalho and Colodette [12] compared the preparation of CNCs by sulfuric acid hydrolysis and sonication method. The needle-shaped CNCs with approximately 200 nm in length and 10 nm in diameter were obtained using a 64 wt% sulfuric acid hydrolysis at 45 °C for 60 min, whereas the microfibrillated celluloses with 20-30 nm in diameter were obtained by using the sonication method. In the same

*Corresponding author. Tel.: +66 4336 2240
Email address: khanita@kku.ac.th
doi: 10.14456/easr.2022.73

way, Tonoli et al. [13] reported the use of sulfuric acid hydrolysis, refining, and sonication method to prepare cellulose micro/nanofibers. The results showed that the nanofibers obtained from the refining method were on average 30 nm in diameter and 100-450 nm in length, whereas the nanofibers from the sonication method were in the range of 20-50 nm in diameter and 200 to 2,500 nm in length. For the sulfuric acid hydrolysis, the crystalline rod-like nanofibers (whiskers) with approximately 142 nm in length and 11 nm in diameter were obtained at a sulfuric acid concentration of 60 %v/v at 45 °C for 60 min. The maximum crystallinity index was obtained by sulfuric acid hydrolysis [14]. It should be noted that acid hydrolysis can be used to produce highly crystalline particles due to the amorphous celluloses being removed and also the size of CNCs being reduced. Meanwhile, the obtained nanofibril from the mechanical methods had low tensile strength due to the amorphous regions remaining in its structure, which were weak and easy to break down. For these reasons, sulfuric acid hydrolysis is considered the method with high potential to be used in producing CNCs. However, *Eucalyptus* species grown in different areas with variations in soil, weather, and groundwater levels may affect the chemical composition, morphology, and mechanical strength of the *Eucalyptus* pulp [2, 15].

Eucalyptus pulp is one of the high cellulose sources which could be extracted from highly crystalline regions. However, the effect of CNCs preparation from *Eucalyptus* pulp in hydrolysis conditions on the obtained particle structure in nano or microcrystalline cellulose is required to understand, which can be applied in various specific applications. Furthermore, the CNC production from *Eucalyptus* pulp is an alternative way to produce a more sustainable material in the paper industry. Determining the optimal condition to synthesize CNCs from the *Eucalyptus* pulp would be an alternative way to add value to the pulp. Therefore, identifying the best preparation condition for the production of CNCs from the *Eucalyptus* pulp in the northeast of Thailand is crucial in this study. The effects of operating factors, including sulfuric acid concentration, temperature, and hydrolysis time, on CNC production were studied simultaneously to obtain the optimal condition for producing high-quality CNCs. In addition, as-prepared CNCs were compared with CNCs from other reports. This research provided an alternative way to use *Eucalyptus* pulp feedstock for cellulose nanocrystal production.

2. Materials and methods

2.1. Materials

Eucalyptus pulp sheets were provided by Phoenix Pulp and Paper Public Com. Ltd. Sulfuric acid aqueous solution (96 wt%) was supplied by RCI Labscan (Thailand). All experimental solutions were prepared using deionized (DI) water.

2.2 CNC Preparation

In preparing the CNCs, the *Eucalyptus* pulp was crushed, and then it was passed through a sieve (40 mesh). CNCs were prepared following the method described in our previous work [4]. Briefly, 1 g of sieved pulp was mixed with 20 ml of various sulfuric acid concentrations. The mixed solution was sonicated for 15 minutes before it was hydrolyzed at various temperatures and for different time durations. After that, the residual solid phase in the mixed solution was separated by means of a centrifuge at 9,000 rpm. The residual was then washed with distilled water until neutralized. The conditions of hydrolysis were predetermined to be as follows: sulfuric acid concentrations at 30, 40, and 50 wt%; hydrolysis temperatures at 60, 70, and 80 °C; and hydrolysis durations for 30, 60, and 90 min. The CNC samples were named according to the preparation conditions; for example, CNCs 30-60-60 meant the CNCs were produced by using a sulfuric acid concentration of 30 wt%, hydrolysis temperatures of 60 °C, and hydrolysis time for 60 minutes.

2.3 Characterization of CNCs

2.3.1 XRD

The crystallinity index (CI) and crystalline sizes were analyzed via X-ray diffraction (XRD, Bruker D8 Advance, Germany). The CNCs were scanned within 2θ of 5-50°. The crystal profile of cellulose models was drawn using Mercury software 4.3.1 (The Cambridge Crystallographic Data Centre Cambridge, UK). The XRD pattern intensity and the maximum intensity of cellulose were used to calculate the crystallinity index according to the empirical method of Segal et al. [16].

$$C_{Ir}(\%) = \frac{(I_{200} - I_{am})}{I_{200}}\ x\ 100 \quad (1)$$

where I_{200} is the maximum intensity of the principal peak lattice diffraction ($2\theta = 22.5$) and I_{am} is the intensity of diffraction attributed to amorphous celluloses ($2\theta = 18°$).

The crystalline size was calculated based on Scherrer equation, as shown in Equation (2).

$$\tau = \frac{K\lambda}{\beta cos\theta} \quad (2)$$

where τ is the mean size of the ordered crystalline, K is a dimensionless shape factor, λ is the X-ray wavelength, β is half of the maximum intensity (FWHM), and θ is the Bragg angle.

2.3.2 Fourier-transform infrared spectroscopy (FT-IR)

Functional groups of CNCs and *Eucalyptus* pulp were investigated using FT-IR spectrometer (Bruker, Germany). Ten mg of CNCs and 10 mg of *Eucalyptus* pulp were separately pressed into an acrylic mould with a diameter of 10 mm. The samples were thereafter analyzed in spectral wave numbers between 600 and 4000 cm^{-1} with a 4 cm^{-1} of resolution.

2.3.3 Morphology

Surface morphologies of CNCs and *Eucalyptus* pulp were investigated using scanning electron microscope (SEM) (PANalytical Empyrean, the Netherlands). The samples were placed on the carbon tape and then coated with gold using a vacuum sputter coater (VTC-16-3HD-LD, USA). The SEM was used with 100 and 1000 magnification with an acceleration voltage of 5.00 kV.

A transmission electron microscope (TEM) (Tecnai 12, Philips, Holland) was used to determine the dimension of CNCs and *Eucalyptus* pulp samples. The samples were dispersed in ethanol in a ratio of 1:100 (mg of samples: mL of ethanol). In total, 10 µl of samples were dropped onto the carbon-coated electron microscopy grid. The sample grids were thereafter observed at 100 kV using a transmission electron microscope.

2.3.4 Thermal gravimetric analysis (TGA)

A TG analysis (TGA 50, Shimadzu, Japan) was performed to determine the thermal decomposition of CNCs and *Eucalyptus* pulp. For this analysis, 10 mg of samples were used in the thermal decomposition analysis. Thermal gravimetric measurements were performed from 25 to 600 ℃ at a constant heating rate of 10 ℃ per min. All measurements were taken under a pure nitrogen gas flow of 10 ml per min. The obtained results were used to calculate a differential thermal gravimetric analysis (DTGA).

3. Results and discussion

3.1 Crystallinity index (%CrI) and crystalline size

The effects of the concentration of sulfuric acid, temperature, and hydrolysis time on crystalline profiles of CNCs were investigated using XRD. XRD profiles of *Eucalyptus* pulp and CNCs with the crystalline structure of cellulose type I are shown in Figure 1. All samples exhibited peaks of 2θ values at approximately 15°, 16°, 22°, and 34.5°, which corresponded to the (110), $(1\bar{1}0)$, (200), and (004) lattice planes, respectively [14]. From the XRD patterns, the peaks at 2θ values of approximately 15°-16° of CNCs became lower than that of the *Eucalyptus* pulp, and the intensity of CNCs was noted to decrease with an increase in sulfuric acid concentration. This indicated that the (110) and $(1\bar{1}0)$ planes corresponded to hydrogen bond between macromolecular chains, and the (110) plane consisted of high OH groups, which were highly susceptible during acid hydrolysis [17]. The (200) plane at 2θ = 22.7° included a glucopyranose link forming the macromolecular chain, and it contained the highest density of electrons, which then resulted in the highest intensity in XRD patterns [18, 19]. The (200) plane of CNCs became lower than that of *Eucalyptus* pulp, which was caused by the hydrolysis reaction with a high concentration of sulfuric acid (50 wt%) and long hydrolysis time (60-90 min). It can be associated with a likely change in the orientation of cellulose chains due to the harsh hydrolysis conditions; in fact, similar results were found in several studies such as Vasconcelos et al.[20], and de Carvalho Benini et al. [17]. The small peak at 2θ = 34.5° corresponded to the (004) lattice plane [13], and it remained constant in all XRD patterns. This behavior indicated that the (004) plane was not affected by acid hydrolysis. The number of crystalline structures in cellulosic materials was indicated by the parameter of %CrI. Figure 2 (a) shows the effect of sulfuric acid concentration and hydrolysis temperature on %CrI, with a fixed hydrolysis time of 60 min. As per the results, it was found that %CrI gradually increased with increasing sulfuric acid concentration at a temperature of 60 ℃. The increase of sulfuric acid concentration from 30 to 50 wt% resulted in an increase of the %CrI of CNCs from 71.55 ± 1.42 to 75.55 ± 1.51. It can be inferred that the increase of sulfuric acid concentration can resulted in increased crystallinity due to higher solubilization of the amorphous regions. This result is in accordance with the intensity of the diffraction planes (110) and $(1\bar{1}0)$ of the CNCs, which decreased with increasing sulfuric acid concentration.

In contrast, the cases of hydrolysis at temperatures of 70 and 80 ℃ showed a remarkable decrease of %CrI with increasing *sulfuric acid concentration*. It was possible that the optimal point of crystallinity was reached, which then resulted in decreasing crystallinity due to the solubility of crystalline regions [21]. Figure 2(b) shows the effect of sulfuric acid concentration and hydrolysis time on %CrI, with a fixed hydrolysis temperature at 60 ℃. *The results showed that hydrolysis time had a slight effect on* %CrI *at a sulfuric concentration of 30 and 40 wt%. While* at *the sulfuric concentration of 50 wt%, CNCs with* short hydrolysis time had a significant difference in %CrI from those with long hydrolysis time. The maximum % CrI of 75.51 ± 1.51 was obtained at the hydrolysis time of 60 min, whereas CNCs with %CrI of 72.11 ± 1.44 and 68.43 ± 1.36 was obtained by using hydrolysis time of 30 min and 90 min, respectively. The increase of %CrI when the hydrolysis time changed from 30-60 min was due to the removal of amorphous regions [22]. It is thus important to note that the hydrolysis time of 90 min yielded the lowest %CrI. It was possible that the damage to the crystalline structure occurred during the long hydrolysis time. It should be noted that all the CNCs had % CrI higher than that of the *Eucalyptus* pulp (65.96% ± 1.26%), which indicated that acid hydrolysis could be a potential method to produce the CNCs.

Figure 3(a) shows the effects of sulfuric acid concentration and hydrolysis temperature on the crystalline size of the CNCs, with a fixed hydrolysis time of 60 min. It was observed that the crystalline size of the CNCs decreased with increasing sulfuric acid concentration. In the case of hydrolysis temperature of 80 ℃, CNCs exhibited a dramatic decrease in crystallite size with increasing *sulfuric acid concentration*. At the sulfuric acid concentration of 50 wt% and the hydrolysis temperatures of 70 and 80 ℃, the crystalline size could not be determined because the hydrolysis temperature >60 ℃ was deemed unsuitable for the preparation of the CNCs due to the decomposition of the crystalline regions. Figure 3(b) shows the effects of sulfuric acid concentration and hydrolysis time on the crystalline size of CNCs, with a fixed hydrolysis temperature of 60 ℃. The results showed that the crystalline size tended to be smaller when produced under a high concentration of sulfuric acid and long hydrolysis time. The smallest crystalline size of 4.03 nm was obtained by using a sulfuric acid concentration of 50 wt% at the hydrolysis time of 60 min. This result was similar to that reported by Merlini et al. (2018), who determined the crystalline size of cellulose type I in the range of 4.0-4.6 nm in diameter by using the sulfuric acid concentration of 50 wt% and the hydrolysis temperature of 45 ℃ with the hydrolysis time in the range of 20-30 min [21]. These CNCs of small crystalline size and high crystallinity may be used as an alternative material for smart windows or LED display production with cellulose type I [23]. The crystal structure of cellulose I is consistent with natural cellulose, as evidenced by the unfragmented peak plane (200) [24].

Generally, four crystalline forms of cellulose were found. Cellulose I is found in its natural form. Cellulose II and III can be prepared by treating cellulose I with NaOH and liquid ammonia, and cellulose IV is obtained by heating cellulose III [25]. During the acid hydrolysis process, the amorphous region was eliminated from the cellulose structure more easily than the crystal region by hydronium ions from the acid solution. It has been reported that cellulose I is considered more suitable for use as a nanomaterial among other cellulose types, as it is the most abundant of stable parallel cellulose chains [26].

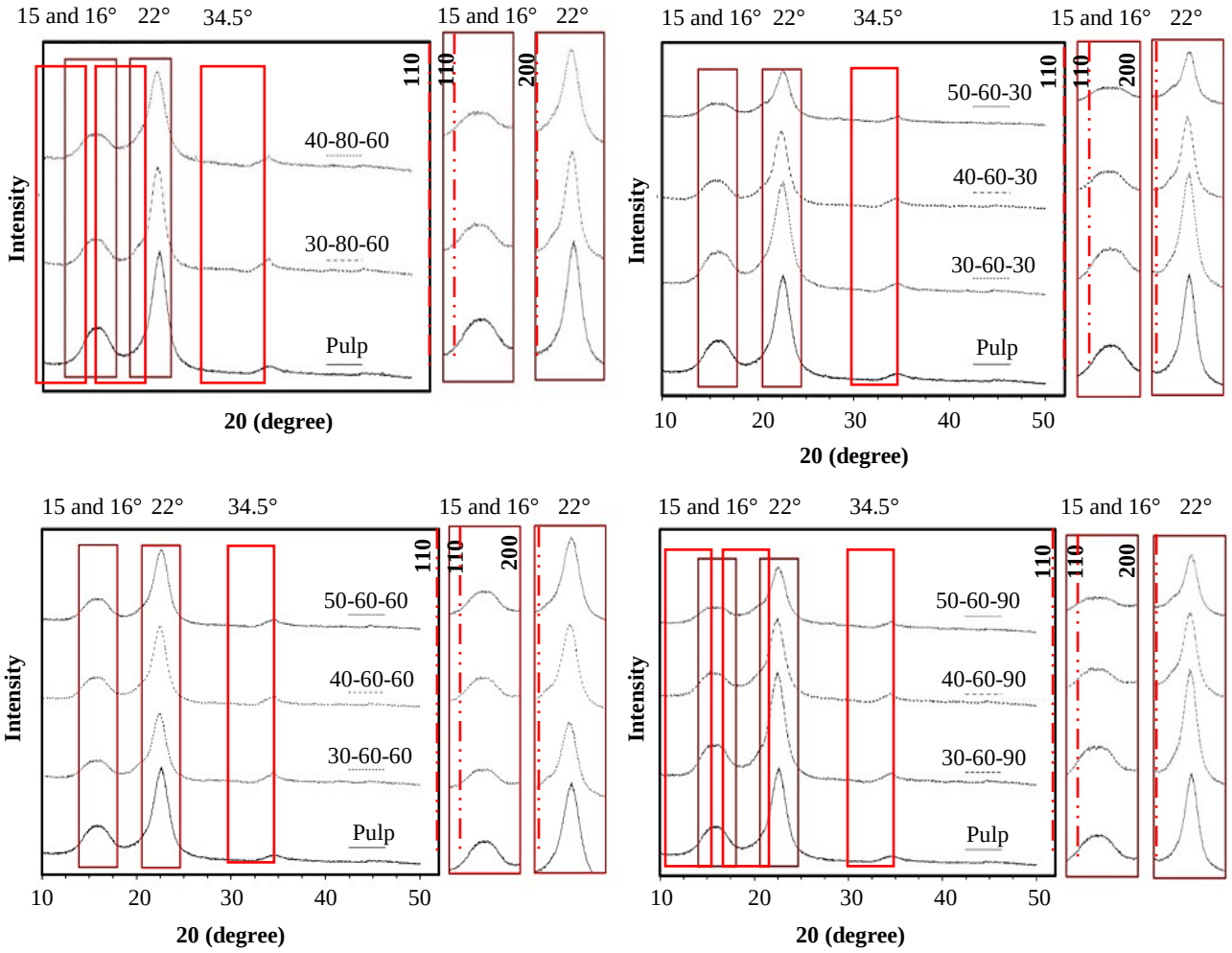

Figure 1 The XRD patterns of *Eucalyptus* pulp and the CNCs obtained from various sulfuric acid concentrations, temperature, and hydrolysis time.

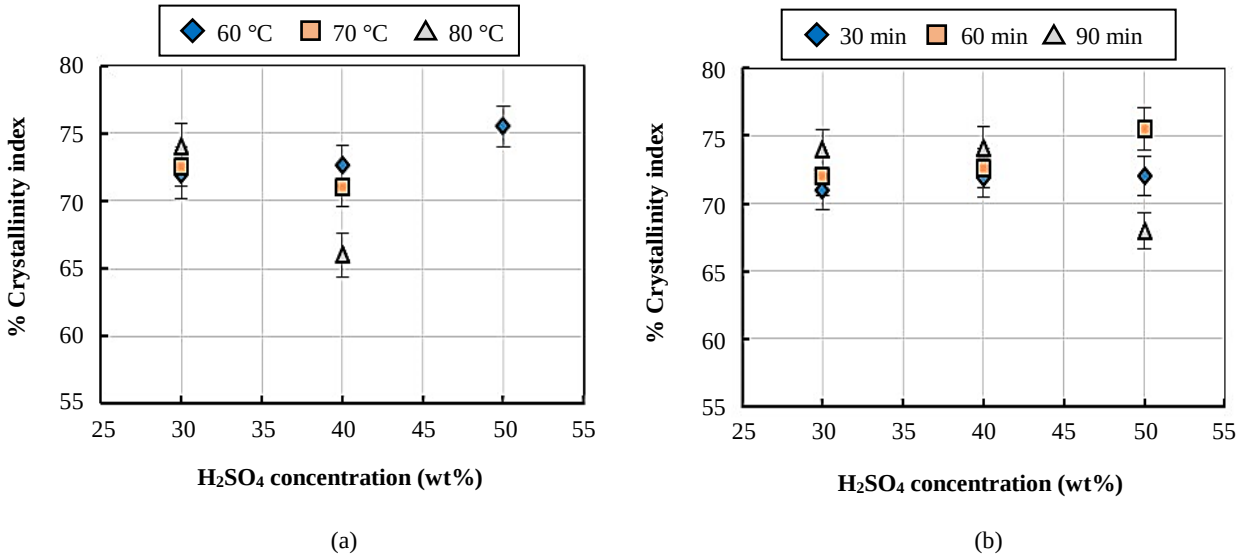

Figure 2 A crystallinity index (%CrI) of CNCs. (a) Effect of sulfuric acid concentration and hydrolysis temperature on %CrI, with a fixed hydrolysis time at 60 min. (b) Effect of sulfuric acid concentration and hydrolysis time on %CrI, with a fixed hydrolysis temperature at 60 °C.

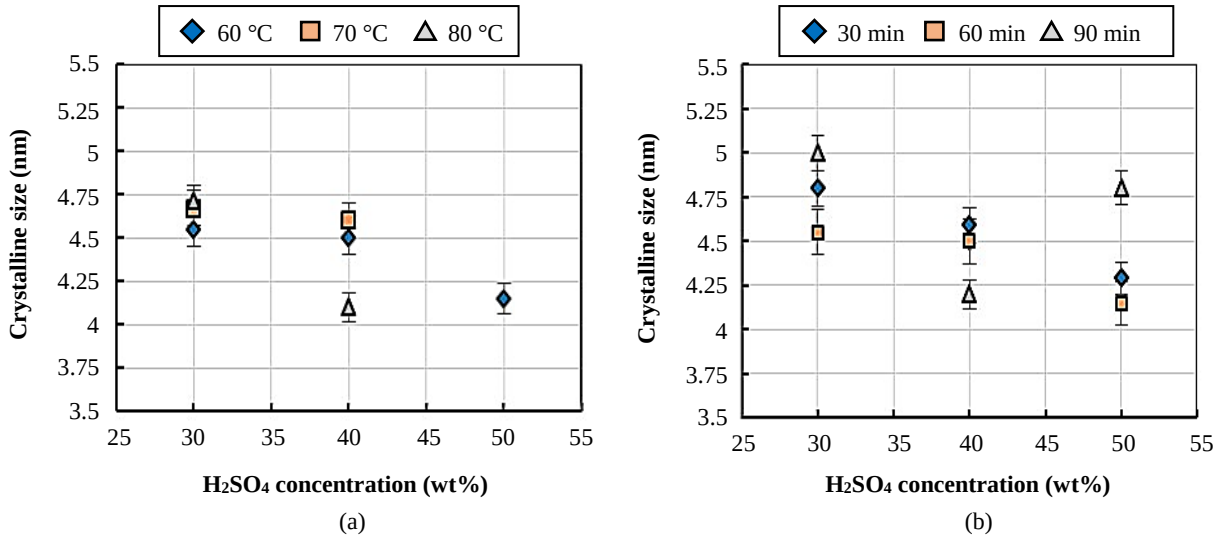

Figure 3 A crystalline size of CNCs. (a) Effect of sulfuric acid concentration and hydrolysis temperature on crystalline size, with a fixed hydrolysis time at 60 min. (b) Effect of sulfuric acid concentration and hydrolysis temperature on crystalline size, with a fixed hydrolysis temperature at 60 °C.

3.2 FT-IR Results

Figure 4 shows a FT-IR spectrum of the CNCs prepared from *Eucalyptus* pulp using sulfuric acid concentrations of 30, 40, and 50% wt with the hydrolysis temperature of 60 °C for the hydrolysis time of 60 min. As per the results, good resemblances of the spectra of the CNCs and the *Eucalyptus* pulp were determined. The intensity peaks at 3330 and 1028 cm^{-1} were associated with the hydroxyl group (OH) stretching due to the vibration of the hydroxyl group (OH) bond, which indicated the hydrophilic tendency of the fibers [26].

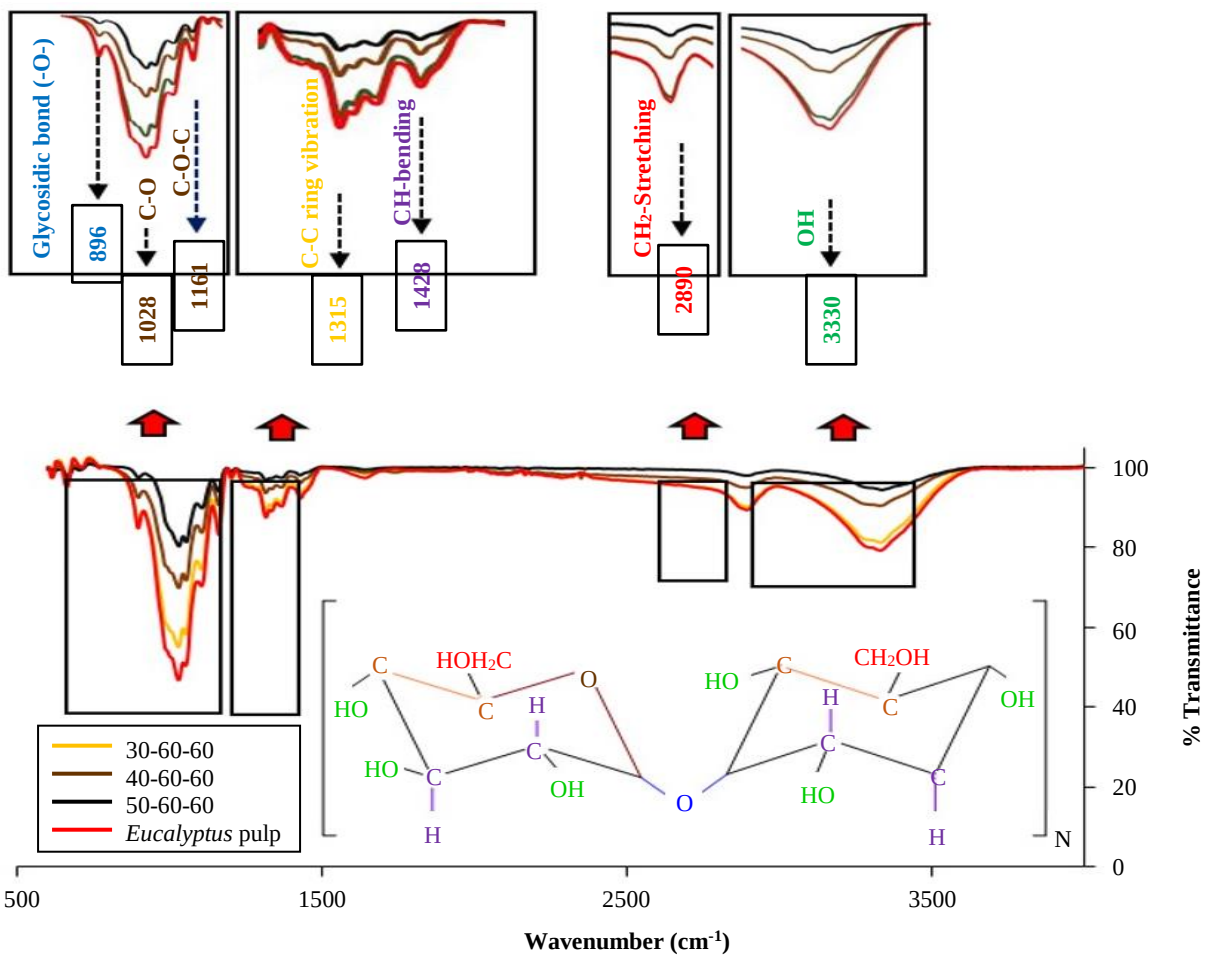

Figure 4 FT-IR Spectra of the CNCs prepared from the *Eucalyptus* pulp using sulfuric acid concentrations of 30, 40, and 50 %wt with hydrolysis temperature of 60 °C and hydrolysis time of 60 min.

The peak at 2890 cm^{-1} was associated with the symmetric and antisymmetric stretching of C-H in methyl (CH_2) and methylene (CH_3) groups [8]. The peak at 1640 cm^{-1} was associated with the stretching vibration of $^{-}$OH, which could be the bending mode of the absorbed water and could have attributed to the carboxylate groups. The CH bending, the stretching of C-C ring vibration, and the stretching of C-O-C linkages in the glucosidic rings also appeared at 1428, 1315, and 1161 cm^{-1}, respectively [27]. The increase in C-O-C asymmetric stretching of the cellulose was indicated by the increase in the intensity of this particular peak. The increase of the peak suggested greater conversion of the *Eucalyptus* pulp to the CNCs. [28]. The appearance of the peaks at 1051 to 1028 cm^{-1} was associated with C-O stretching in the C-O-C pyranose ring skeleton in the cellulose fiber [29]. The spectrum at 896 cm^{-1} was associated with ß-glycosidic linkages between the glucose in cellulose. Remarkably, the intensity of peaks at 1028 and 896 cm^{-1} was observed to decrease *with* the increase of sulfuric acid concentration. This could be due to the rupture of the glucosidic rings and glycosidic linkages [30]. A comparison of the spectra between the *Eucalyptus* pulp and the CNCs indicated that the intensity of peaks of the CNCs was lower than that of *the Eucalyptus* pulp spectra. The results indicated that the structure of the cellulose in the *Eucalyptus* pulp might have been oxidized to nanocrystals during the hydrolysis reaction, as shown in Figure 5.

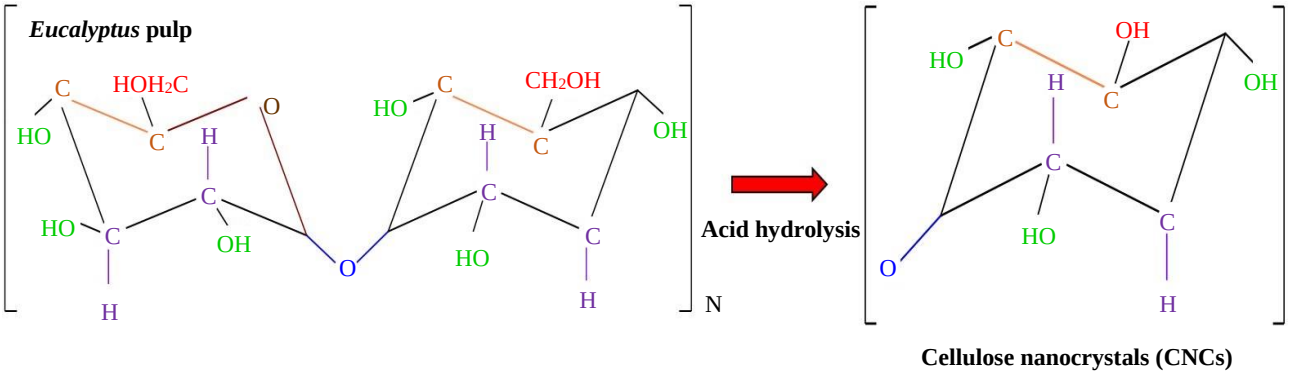

Figure 5 H_2SO_4 Hydrolysis reaction of *Eucalyptus* pulp

3.3 Morphology

The effects of sulfuric acid concentration (30, 40, and 50 wt%) on the surface morphology of the *Eucalyptus* pulp at the temperature of 60 °C with a hydrolysis time of 60 minutes are shown in Figures 6(b)-(d). A comparison of the SEM images between the CNC samples and the *Eucalyptus* pulp (Figure 6(a)) illustrated the particle size of the *Eucalyptus* pulp was longer than that of the CNCs, indicating that the amorphous region was destroyed during the acid hydrolysis process [31]. Sulfuric acid concentration has also affected the morphology of the obtained CNCs, as revealed in Figures 6(b)-(d). The result showed that the fiber length decreased with the increase in sulfuric acid concentration. Figure 6(d) shows the aggregated CNCs, indicating that the amorphous region was also destroyed during the acid hydrolysis process, as revealed by the intensity of CO and CH peaks in the CNC spectra. In the case of hydrolysis using the sulfuric acid concentration of 50 %wt, the aggregation of cellulose structure occurred after the drying process. During the drying process, water was removed from the gel structure, yielding a solid-like gel structure [32].

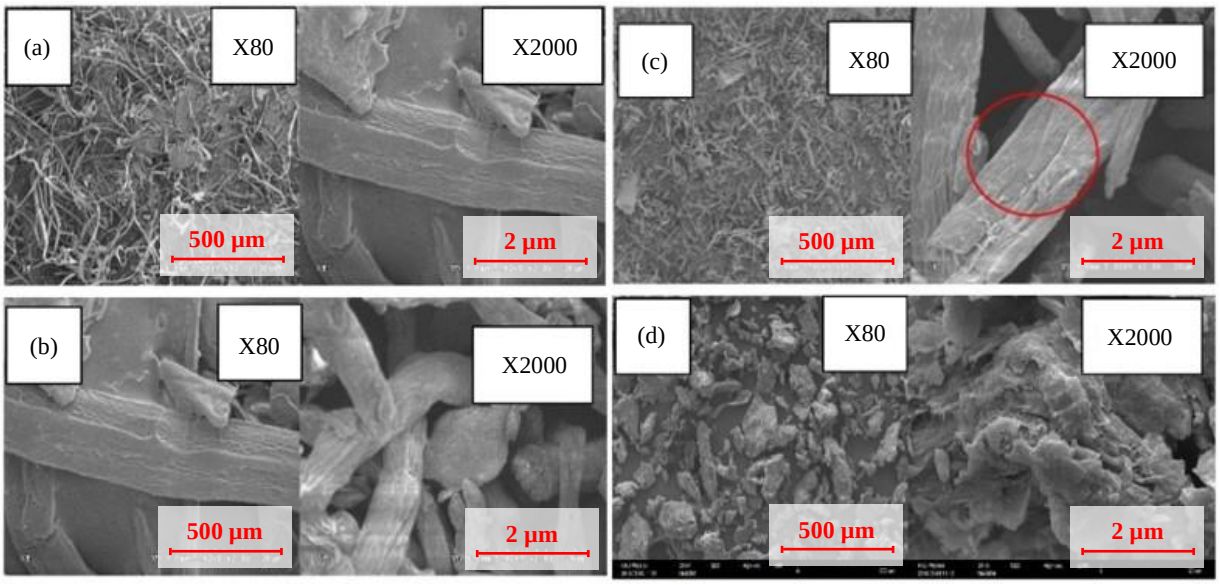

Figure 6 SEM Images of *Eucalyptus* pulp and cellulose nanocrystal with magnification at 80 and 2000 X, (a): *Eucalyptus* pulp (b): CNCs with 30 %wt, (c): CNCs with 40%wt, and (d): CNCs with 50%wt of H_2SO_4, the temperature at 60 °C and hydrolysis time of 60 min.

Figure 7 Shows the TEM images of *Eucalyptus* pulp and CNCs. As shown in Figure 7(a), the length of the *Eucalyptus* pulp was approximately 50-500 µm. In CNCs synthesized using the sulfuric acid concentration of 50 %wt with the temperature of 60 °C with the hydrolysis time of 60 min, the rod-like structure of CNCs was found. The particles of CNCs were approximately 12-25 nm, as shown in Figure 7(b).

In this study, the effects of acid hydrolysis on the *Eucalyptus* pulp structure could be clearly observed by using the sulfuric acid concentration of 50 %wt. It should be noted that the cellulose nanocrystals were found using the sulfuric acid concentration of 50 wt%. In this condition, the glycoside bonds in the amorphous region of cellulose were broken, and the cellulose nanocrystals were released from the cellulose [33]. In addition, this condition gave a higher chance to create the nanoparticles of 500-1000 nm in length, as reported by Tonoli et al. [14], who found that the length of cellulose nanofibers from bleached *Eucalyptus* pulp was approximately 800 nm and the morphology of the cellulose nanofibers after acid hydrolysis was similar in the form of rods.

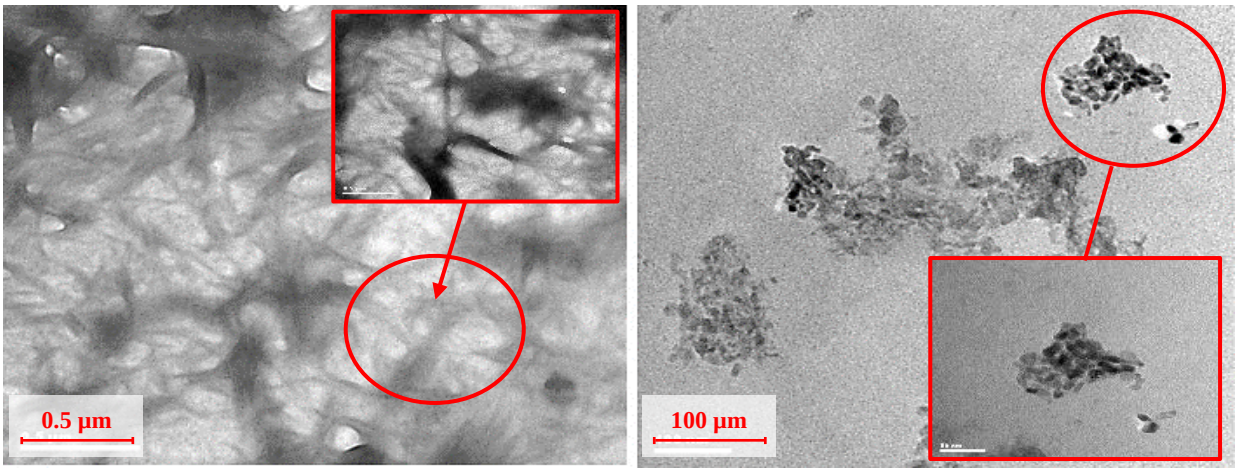

(a) (b)

Figure 7 TEM Images of *Eucalyptus* pulp (a) and CNCs (b) from 50% sulfuric acid concentration with the temperature of 60 °C for hydrolysis time at 60 minutes.

3.4 Thermal gravimetric analysis

Figure 8(a) shows the TGA curves of *Eucalyptus* pulp and CNCs after acid hydrolysis with sulfuric acid concentrations of 30, 40, and 50 wt%, hydrolysis temperature of 60 °C, and hydrolysis time at 60 minutes. The TGA curves of the *Eucalyptus* pulp showed the three stages of decomposition, and so did the TGA curves of the hydrolyzed *Eucalyptus* pulp.

The first decomposition stage was the evaporation of moisture between temperatures of 25 and 125°C. All samples displayed an initial small amount of weight loss during this stage. This stage corresponds to the evaporation of water from the surface of the cellulose [34].

The second stage took place at a temperature between 200 and 350°C. During this stage, the weight loss of the *Eucalyptus* pulp was noted to be slow, and the total weight loss percentage was approximately 80%. In the CNCs, the weight loss was approximately 60%. In the CNCs using the sulfuric acid concentration of 50 %wt, the degradation of small crystals at temperatures between 150 and 300°C [29] was found in our previous work. A similar result was reported by Jiang and Hsieh [35], who found that the cellulose nanocrystal showed low thermal stability during the temperatures between 200 and 350 °C.

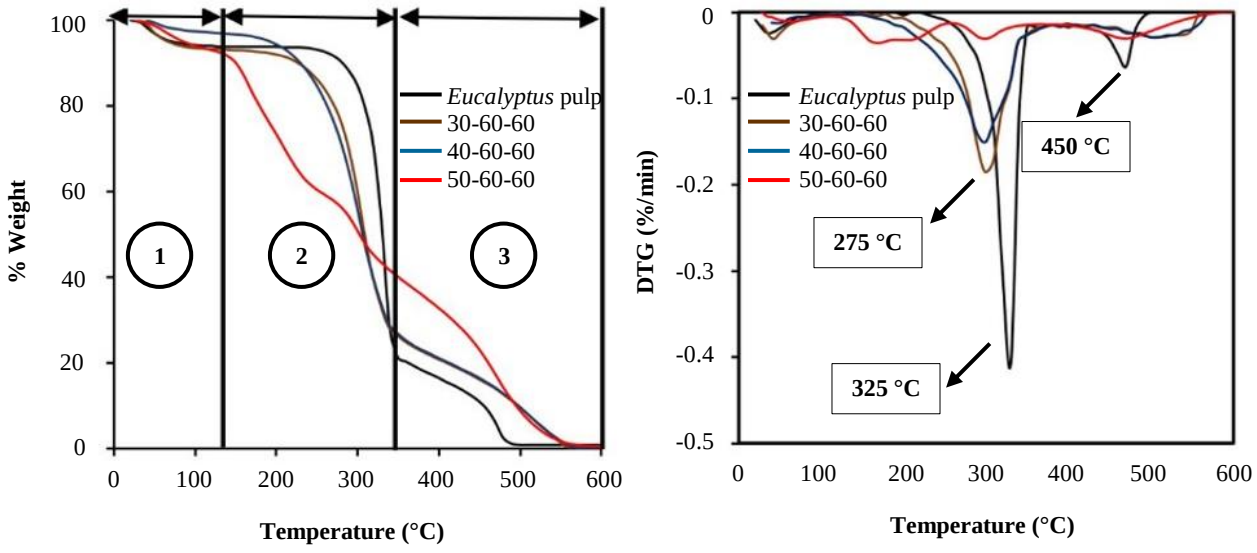

(a) TGA (b) DTGA

Figure 8 (a) TGA curves of *Eucalyptus* pulp and CNCs by sulfuric concentrations 30, 40, and 50 %wt with hydrolysis temperature of 60 °C and hydrolysis time of 60 min. (b) DTGA curves of *Eucalyptus* pulp and CNCs with the same hydrolysis conditions as those of the TGA curves

At the last stage, where the temperature was between 350 and 600°C, the weight of *Eucalyptus* pulp gradually decreased, and it was transformed into ashes at the temperature of 500 °C. In contrast, the CNCs showed high thermal stability at the temperature between 350 and 550 °C. The residual weight of the CNCs was approximately 40% at the temperature of 400°C. This result is consistent with the findings of Voronova et al. [29], who reported that the cellulose nanocrystal showed stability of thermal decomposition due to the compact and high-density structure of cellulose nanocrystals. At the temperature of 500 °C, the residual weight of *Eucalyptus* pulp was approximately 8%, whereas the residual weight of CNCs was approximately 15%. This could be due to the amorphous region of cellulose which was destroyed by acid hydrolysis. Moreover, the presence of nanocrystals caused the CNCs to have more thermal stability than the amorphous region [36]. This is because of the sulfate ester groups of the crystalline regions, which have flame-resistant characteristics [37].

Figure 8(b) shows a DTGA of the *Eucalyptus* pulp and the CNCs using sulfuric acid concentrations of 30, 40, and 50 %wt. It can be confirmed that the amorphous region of the cellulose was decomposed at temperatures between 300 and 350 °C [38], whereas the decomposition of CNCs occurred at temperatures between 250 and 350 °C. This result could be explained by the presence of the carboxyl and sulfate groups. These groups were generated by a hydrolysis reaction, and they can be easily decomposed at temperatures below 300 °C [38], and also an orderly crystal structure lends itself to faster and easier heat transmission than an irregular structure. Crystalline structures, therefore, undergo thermal decomposition at lower temperatures than amorphous structures.

3.5 Conceptual idea for pulp and paper valorization process

Figure 9 shows a conceptual idea for the valorization process in pulp and paper manufacturing. Basic pulp and paper manufacturing involves four steps [39], namely, preparation of raw material, kraft pulp, bleaching process, and papermaking procedure.

Firstly, the *Eucalyptus* wood is mechanically chopped into small pieces, often referred as chips. Secondly, the chips are then cooked in a digester to separate the fiber from the chips. In this step, sodium hydroxide and sodium sulfide are added. Lignin is removed by the chemical reaction [40]. After that, the cooked pulp is returned to the chemical recovery cycle. Thirdly, the separated fiber is passed through a bleaching process. The fiber was further dignified by chlorination and oxidation. The last step is the papermaking process. The bleached pulp is fed to the press machine, where the remaining water in the pulp is removed by heated cylinders.

The result of our work suggests there is an opportunity to increase the value of the *Eucalyptus* pulp by a process which can be integrated to the existing processes of the industry, as illustrated in Figure 9. The integral process will lead to a solution to the environmental and economic problem by using the inexpensive pulp to produce high-valued nanomaterials and recovering the needed sulfuric acid from the pulping process. The sulfuric acid for cellulose nanocrystal production can be obtained by the wet gas sulfuric acid (WSA) process. During the WSA process, commercial-grade sulfuric acid (95%-98%wt.) can be derived from a pulp mill process with condensable gases [41]**.** The sulfuric acid is generated from what is otherwise air pollution as sulfur dioxide in an incinerator [42]. The reaction of sulfuric acid generation is shown in the equations below.

$$H_2O + 1.5\ O_2 \rightarrow SO_2 + H_2O \quad (3)$$

$$SO_2 + 0.5\ O_2 \rightarrow SO_3 \quad (4)$$

$$SO_3 + H_2O \rightarrow H_2SO_4\ (g) \quad (5)$$

$$H_2SO_4\ (g) \rightarrow H_2SO_4\ (l) \quad (6)$$

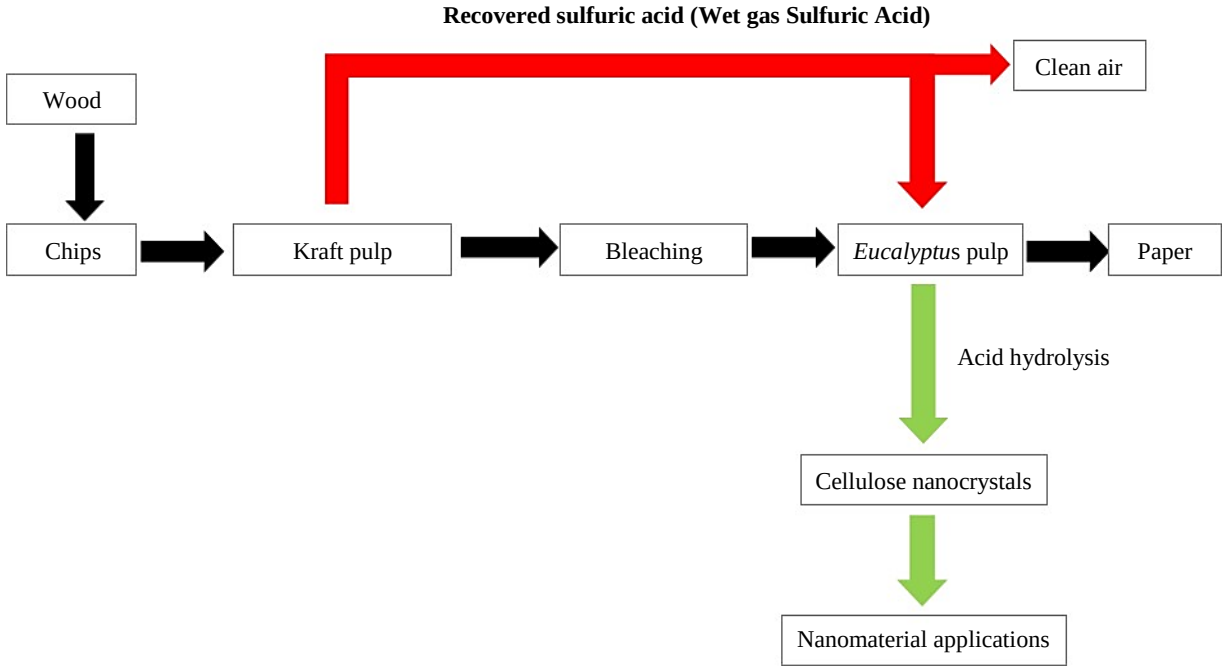

Figure 9 Conceptual ideal for valorization process in pulp and paper manufacturing.

4. Conclusion

We have synthesized CNCs from *Eucalyptus* pulp by sulfuric acid hydrolysis to find an alternative way to produce value-added feedstock from abundantly available *Eucalyptus* pulp. We used *Eucalyptus* pulp as a raw material for CNC production. The effects of H_2SO_4 concentration, hydrolysis time, and hydrolysis temperature were investigated to determine the best condition to prepare CNCs. As per our findings, it was found that an increase in H_2SO_4 concentration, time, and temperature can lead to a lower percentage of crystallinity and reduced crystal size; this entails that crystallinity percentage and CNC particle size can be controlled for each specific application. The physical and chemical characteristics of cellulose nanocrystals were analyzed using X-ray diffraction, scanning electron microscope (SEM), Fourier-transform infrared spectroscopy (FT-IR) and TGA. The best hydrolysis condition was determined at 50 %wt of the sulfuric acid concentration, 60°C hydrolysis temperature, and hydrolysis time of 60 min. At this condition, the crystallinity as high as $75.5\% \pm 1.51\%$ and an average crystal size of 4.03 ± 0.10 nm were achieved. The FT-IR result illustrated a decrease in the amorphous region of the *Eucalyptus* pulp resulting in the high crystallinity of the cellulose nanocrystals. The thermal stability of the modified cellulose nanocrystals was examined by TGA analysis. Furthermore, the CNC properties from *Eucalyptus* pulp in this study suggested the high crystallinity percentage and the smallest crystalline size in nanoscale, which would be applied to various cosmetic and pharmaceutical commercial applications. In addition, the synthesized CNCs from *Eucalyptus* pulp have the potential for valorization of pulp to CNCs in the paper industry.

5. Acknowledgement

The authors would like to give gratitude and acknowledge to the "Research and Graduate Studies" Khon Kaen University for their supports and the Graduate School at Khon Kaen University for student financial support. We are also grateful to the Department of Separation Science at Lappeenranta University of technology for supporting characterized instruments.

6. References

[1] Jutakridsada P, Pimsawat N, Sillanpää M, Kamwilaisak K. Olive oil stability in Pickering emulsion preparation from *Eucalyptus* pulp and its rheology behaviour. Cellulose. 2020;27(11):6189-203.
[2] Jutakridsada P, Iamamornphanth W, Patikarnmonthon N, Kamwilaisak K. Usage of *Eucalyptus globulus* bark as a raw material for natural antioxidant and fuel source. Clean Technol Environ Policy. 2017;19(3):907-15.
[3] Liu J, Willför S, Mihranyan A. On importance of impurities, potential leachables and extractables in algal nanocellulose for biomedical use. Carbohydr Polym. 2017;172:11-9.
[4] Kamwilaisak K, Pimsawat N, Khotsakha N, Jutakridsada P. Synthesis and characterization of cellulose nanocrystal from *Eucalyptus* pulp. N Biotechnol. 2018;44:S97.
[5] Fleming K, Gray DG, Matthews S. Cellulose crystallites. Chem Eur J. 2001;7(9):1831-6.
[6] Habibi Y, Lucia LA, Rojas OJ. Cellulose nanocrystals: chemistry, self-assembly, and applications. Chem Rev. 2010;110(6):3479-500.
[7] Huang S, Li S, Lu X, Wang Y. Modification of cellulose nanocrystals as antibacterial nanofillers to fabricate rechargeable nanocomposite films for active packaging. ACS Sustainable Chem Eng. 2022;10(28):9265-74.
[8] Zhao J, He X, Wang Y, Zhang W, Zhang X, Zhang X, et al. Reinforcement of all-cellulose nanocomposite films using native cellulose nanofibrils. Carbohydr Polym. 2014;104:143-50.
[9] Besbes I, Alila S, Boufi S. Nanofibrillated cellulose from TEMPO-oxidized *Eucalyptus* fibres: effect of the carboxyl content. Carbohydr Polym. 2011;84(3):975-83.
[10] Ruiz-Caldas MX, Carlsson J, Sadiktsis I, Jaworski A, Nilsson U, Mathew AP. Cellulose nanocrystals from postconsumer cotton and blended fabrics: a study on their properties, chemical composition, and process efficiency. ACS Sustainable Chem Eng. 2022;10(11):3787-98.
[11] Spinella S, Maiorana A, Qian Q, Dawson NJ, Hepworth V, McCallum SA, et al. Concurrent cellulose hydrolysis and esterification to prepare a surface-modified cellulose nanocrystal decorated with carboxylic acid moieties. ACS Sustainable Chem Eng. 2016;4(3):1538-50.
[12] de Carvalho DM, Colodette JL. Comparative study of acid hydrolysis of lignin and polysaccharides in biomasses. Bioresources. 2017;12(4):6907-23.
[13] Tonoli G, Holtman KM, Glenn G, Fonseca AS, Wood D, Williams T, et al. Properties of cellulose micro/nanofibers obtained from *Eucalyptus* pulp fiber treated with anaerobic digestate and high shear mixing. Cellulose. 2016;23(2):1239-56.
[14] Tonoli GHD, Teixeira EM, Corrêa AC, Marconcini JM, Caixeta LA, Pereira-da-Silva MA, et al. Cellulose micro/nanofibres from *Eucalyptus* kraft pulp: preparation and properties. Carbohydr Polym. 2012;89(1):80-8.
[15] Dutt D, Tyagi CH. Comparison of various *Eucalyptus* species for their morphological, chemical, pulp and paper making characteristics. Indian J Chem Technol. 2011;18:145-51.
[16] Segal L, Creely JJ, Martin AE, Conrad CM. An empirical method for estimating the degree of crystallinity of native cellulose using the X-ray diffractometer. Text Res J. 1959;29(10):786-94.
[17] de Carvalho Benini KCC, Voorwald HJC, Cioffi MOH, Rezende MC, Arantes V. Preparation of nanocellulose from *Imperata brasiliensis* grass using Taguchi method. Carbohydr Polym. 2018;192:337-46.
[18] Ling Z, Wang T, Makarem M, Cintrón MS, Cheng HN, Kang X, et al. Effects of ball milling on the structure of cotton cellulose. Cellulose. 2019;26(1):305-28.
[19] López Durán V, Larsson PA, Wagberg L. On the relationship between fibre composition and material properties following periodate oxidation and borohydride reduction of lignocellulosic fibres. Cellulose. 2016;23(6):3495-510.
[20] Vasconcelos NF, Feitosa JP, da Gama FM, Morais JP, Andrade FK, de Souza Filho MS, et al. Bacterial cellulose nanocrystals produced under different hydrolysis conditions: properties and morphological features. Carbohydr Polym. 2017;155:425-31.
[21] Merlini A, de Souza VC, Gomes RM, Coirolo A, Merlini S, Machado RAF. Effects of reaction conditions on the shape and crystalline structure of cellulose nanocrystals. Cellul Chem Technol. 2018;52(5-6):325-35.
[22] Chen L, Wang Q, Hirth K, Baez C, Agarwal UP, Zhu JY. Tailoring the yield and characteristics of wood cellulose nanocrystals (CNC) using concentrated acid hydrolysis. Cellulose. 2015;22(3):1753-62.

[23] Chen H. 3-Lignocellulose biorefinery feedstock engineering. In: Chen H, editor. Lignocellulose biorefinery engineering. Sawston: Woodhead Publishing; 2015. p. 37-86.
[24] Jutakridsada P, Suwannaruang T, Kasemsiri P, Weerapreeyakul N, Knijnenburg JTN, Theerakulpisut S, et al. Controllability, antiproliferative activity, Ag+ release, and flow behavior of silver nanoparticles deposited onto cellulose nanocrystals. Int J Biol Macromol. In press 2022.
[25] Lavoine N, Desloges I, Dufresne A, Bras J. Microfibrillated cellulose-its barrier properties and applications in cellulosic materials: a review. Carbohydr Polym. 2012;90(2):735-64.
[26] Aulin C, Ahola S, Josefsson P, Nishino T, Hirose Y, Österberg M, et al. Nanoscale cellulose films with different crystallinities and mesostructures-their surface properties and interaction with water. Langmuir. 2009;25(13):7675-85.
[27] Matthew IR, Browne RM, Frame JW, Millar BG. Subperiosteal behaviour of alginate and cellulose wound dressing materials. Biomaterials. 1995;16(4):275-8.
[28] Saelee K, Yingkamhaeng N, Nimchua T, Sukyai P. An environmentally friendly xylanase-assisted pretreatment for cellulose nanofibrils isolation from sugarcane bagasse by high-pressure homogenization. Ind Crops Prod. 2016;82:149-60.
[29] Voronova MI, Surov OV, Guseinov SS, Barannikov VP, Zakharov AG. Thermal stability of polyvinyl alcohol/nanocrystalline cellulose composites. Carbohydr Polym. 2015;130:440-7.
[30] Brinchi L, Cotana F, Fortunati E, Kenny JM. Production of nanocrystalline cellulose from lignocellulosic biomass: technology and applications. Carbohydr Polym. 2013;94(1):154-69.
[31] Satarn J, Lamamorphanth W, Kamwilaisak K. Acid hydrolysis from corn stover for reducing sugar. Adv Mat Res. 2014;931:1608-13.
[32] Majoinen J, Kontturi E, Ikkala O, Gray DG. SEM Imaging of chiral nematic films cast from cellulose nanocrystal suspensions. Cellulose. 2012;19(5):1599-605.
[33] Wulandari WT, Rochliadi A, Arcana IM. Nanocellulose prepared by acid hydrolysis of isolated cellulose from sugarcane bagasse. IOP Conf Ser Mater Sci Eng. 2016;107(1):012045.
[34] Voronova MI, Zakharov AG, Kuznetsov OY, Surov OV. The effect of drying technique of nanocellulose dispersions on properties of dried materials. Mater Lett. 2012;68:164-7.
[35] Jiang F, Hsieh YL. Super water absorbing and shape memory nanocellulose aerogels from TEMPO-oxidized cellulose nanofibrils via cyclic freezing-thawing. J Mater Chem A. 2014;2(2):350-9.
[36] Mtibe A, Linganiso LZ, Mathew AP, Oksman K, John MJ, Anandjiwala RD. A comparative study on properties of micro and nanopapers produced from cellulose and cellulose nanofibres. Carbohydr Polym. 2015;118:1-8.
[37] Wang Q, Zhao X, Zhu JY. Kinetics of strong acid hydrolysis of a bleached Kraft pulp for producing cellulose nanocrystals (CNCs). Ind Eng Chem Res. 2014;53(27):11007-14.
[38] Lu P, Hsieh YL. Preparation and properties of cellulose nanocrystals: rods, spheres, and network. Carbohydr Polym. 2010;82(2):329-36.
[39] Azhar Zakir MJ, Ramalingam S, Balasubramanian P, Rathinam A, Sreeram KJ, Rao JR, et al. Innovative material from paper and pulp industry for leather processing. J Clean Prod. 2015;104:436-44.
[40] de Azevedo ARG, Alexandre J, Pessanha LSP, Manhães RDST, de Brito J, Marvila MT. Characterizing the paper industry sludge for environmentally-safe disposal. Waste Manage. 2019;95:43-52.
[41] Husnil YA, Andika R, Lee M. Optimal plant-wide control of the wet sulfuric acid process in an integrated gasification combined cycle power plant. J Process Control. 2019;74:147-59.
[42] Mandeep, Gupta GK, Liu H, Shukla P. Pulp and paper industry-based pollutants, their health hazards and environmental risks. Curr Opin Environ Sci Health. 2019;12:48-56.